Published in final edited form as:
Mech Dev. 2009 October ; 126(10): 791–803. doi:10.1016/j.mod.2009.08.003.

Wnt signaling maintains the notochord fate for progenitor cells and supports the posterior extension of the notochord

Kanako Ukita[1], **Shino Hirahara**[1], **Naoko Oshima**[2], **Yu Imuta**[1], **Aki Yoshimoto**[3], **Chuan-Wei Jang**[4], **Masayuki Oginuma**[5], **Yumiko Saga**[6], **Richard R. Behringer**[4], **Hisato Kondoh**[3], and **Hiroshi Sasaki**[1,7]

[1]Laboratory for Embryonic Induction, RIKEN Center for Developmental Biology, 2-2-3 Minatojima-minamimachi, Chuo, Kobe, Hyogo 650-0047, Japan

[2]Laboratory for Animal Resources and Genetic Engineering, RIKEN Center for Developmental Biology, 2-2-3 Minatojima-minamimachi, Chuo, Kobe, Hyogo 650-0047, Japan

[3]Graduate School of Frontier Biosciences, Osaka University, 1-3, Yamada-oka, Suita, Osaka 565-0871, Japan

[4]Department of Genetics, The University of Texas M.D. Anderson Cancer Center, 1515 Holcombe Blvd., Huston, TX77030, USA

[5]SOKENDAI

[6]National Institute of Genetics, Yata 1111, Mishima 411-8546, Japan

Abstract

The notochord develops from notochord progenitor cells (NPCs) and functions as a major signaling center to regulate trunk and tail development. NPCs are initially specified in the node by Wnt and Nodal signals at the gastrula stage. However, the underlying mechanism that maintains the NPCs throughout embryogenesis to contribute to the posterior extension of the notochord remains unclear. Here, we demonstrate that Wnt signaling in the NPCs is essential for posterior extension of the notochord. Genetic labeling revealed that the *Noto*-expressing cells in the ventral node contribute the NPCs that reside in the tail bud. Robust Wnt signaling in the NPCs was observed during posterior notochord extension. Genetic attenuation of the Wnt signal via notochord-specific *β-catenin* gene ablation resulted in posterior truncation of the notochord. In the NPCs of such mutant embryos, the expression of notochord-specific genes was down-regulated, and an endodermal marker, E-cadherin, was observed. No significant alteration of cell proliferation or apoptosis of the NPCs was detected. Taken together, our data indicate that the NPCs are derived from *Noto*-positive node cells, and are not fully committed to a notochordal fate. Sustained Wnt signaling is required to maintain the NPCs' notochordal fate.

Keywords

Notochord; progenitor cells; Wnt; β-catenin; cell fate specification; CreER; lineage tracing

[7]corresponding author: Hiroshi Sasaki, sasaki@cdb.riken.jp, Tel: (Japan +81)-78-306-3147, Fax: (Japan +81)-77-306-3363

1. Introduction

During mouse embryogenesis, the organizer and its descendant signaling centers play central roles in the establishment of the correct body plan (reviewed in (Davidson and Tam, 2000; Niehrs, 2004; Tam and Behringer, 1997). Among them, the midline mesodermal tissue, the notochord, is the major signaling center controlling trunk and tail development. The notochord expresses both signaling molecules and their antagonists, thereby regulating the differentiation, growth, and patterning of the surrounding tissues (see review by (Cleaver and Krieg, 2001). Development of the notochord proceeds from the anterior toward the posterior through the continuous addition of more-posterior cells in parallel with the posterior extension of the body axis.

The notochord develops from notochord progenitor cells (NPCs), which are initially specified in the ventral layer of the node at the late gastrula stage (Kinder et al., 2001). At later stages, the notochord is formed from the tail bud, which was previously thought to be an undifferentiated blastema (Griffith et al., 1992). However, recent studies in *Xenopus* and mouse have divided the tail bud into sub-domains, each consisting of a distinct cell population that arises during gastrulation (Cambray and Wilson, 2002; Cambray and Wilson, 2007; Gofflot et al., 1997; Gont et al., 1993). They showed with dye labeling and cell transplantation experiments that the NPCs originating from the ventral layer of the node contribute to wide range of the notochord, including the posterior end of the elongating notochord in the tail bud (Cambray and Wilson, 2002; Tam et al., 1997). However, these analyses are limited to the duration of in vitro culture of mouse embryos (48 hours), and it remains unknown whether the cells originating from the ventral node of E7.5 or E8.5 embryos actually contribute to the posterior end of the notochord at E13.5. Recent live imaging of the EGFP-expressing node cells revealed presence of two cell types. The cells within the node undergo convergent extension movements to constitute the trunk notochord, and the peripheral node cells actively migrate towards the posterior (Yamanaka et al., 2007), most likely to generate posterior notochord extension. The absence of the notochord in ectopic tails induced by mimicking the tail organizer activities in *Xenopus* and zebrafish embryos also supports the notion that the organizer (containing the equivalent of the mouse node)-derived NPCs form the entire notochord (Agathon et al., 2003; Beck and Slack, 1999; Beck et al., 2001).

Initial specification of NPCs in the node is achieved cooperatively by Wnt and Nodal signals (Lickert et al., 2002; Vincent et al., 2003; Yamamoto et al., 2001). Although the continuous production of notochord cells by the NPCs is critically important to establish the correct body plan, relatively little is known about the mechanisms by which the NPCs are maintained throughout embryogenesis in the tail bud. Notochord development is governed by a set of transcription factors: Foxa2, Brachyury, and Noto (Abdelkhalek et al., 2004; Ang and Rossant, 1994; Herrmann and Kispert, 1994; Weinstein et al., 1994; Yamanaka et al., 2007). Of these, Foxa2 is essential throughout notochord development; the other two are required only for later or posterior notochord development.

Noto cooperates with Foxa2 in trunk notochord development (Yamanaka et al., 2007). To address the mechanism of notochord development, we have examined the regulatory mechanism of *Foxa2* in the node and notochord (Nishizaki et al., 2001; Sasaki and Hogan, 1996; Sawada et al., 2005). Our analysis identified the node/notochord enhancer and its core element, which is essential for the enhancer activity and sufficient for gene expression in the NPCs. This core element is regulated by the cooperation of a Tead family transcription factor and a second factor, and it is regulated downstream of the Wnt signal (Sawada et al., 2008; Sawada et al., 2005). Therefore, we hypothesized that Wnt signaling regulates the development of NPCs. This hypothesis is partially supported by the absence of a posterior notochord in mice bearing a mutant Wnt ligand (Wnt3a), Wnt receptor (LRP5 or LRP6), or downstream

transcription factor (Lef1 or Tcf1) (Galceran et al., 1999; Kelly et al., 2004; Takada et al., 1994). However, because these mutants completely lack or have abnormal posterior tissues, the role of Wnt signaling in NPC development remains to be established.

Here, we showed by genetic lineage tracing that NPCs of the tail bud originate in the ventral node. Next, we examined the role of Wnt signaling in the posterior notochord extension by conditionally inactivating the *β-catenin* gene in only the notochord, including the NPCs. We demonstrated that Wnt signaling in the NPCs is absolutely essential for the posterior extension of the notochord. We also demonstrated that the developmental fate of NPCs to become notochord is not pre-determined. The role of Wnt signaling in the NPCs is to maintain their notochordal fate throughout the notochord's posterior extension.

2. Results

2.1. NPCs in the tail bud proliferate actively

Previous dye-labeling studies showed that the notochord is formed from NPCs that are initially localized to the ventral node and later move to the posterior end of the notochord in the tail bud (Cambray and Wilson, 2002; Cambray and Wilson, 2007; Tam et al., 1997). Although the continuous increase in notochordal mass predicts active proliferation of the NPCs, earlier studies indicate that these cells proliferate little during the period between embryonic day (E) 7.5 and E8.25, when they are in the ventral node (Bellomo et al., 1996). We therefore re-investigated cell proliferation in the NPC-containing tissues up to E10.5. Consistent with previous observations, only 1% of the E7.75 ventral node cells was labeled with BrdU (Fig. 1A, C). However, at E9.25 and E10.5 respectively, 39% and 24% of the cells at the posterior end of the notochord incorporated BrdU within a two-hour period, indicating the active proliferation of NPCs (Fig. 1B, C). Therefore, cell proliferation is inactive only before E9, after which the NPCs in the tail bud proliferate actively to generate the long-lasting posterior extension of the notochord.

2.2. *Noto*-positive node cells contribute the NPCs of the tail bud, which generate the posterior notochord extension

A recent live-imaging study of $Noto^{+/eGFP}$ knock-in mouse embryos, which express EGFP in the cells of the ventral node and posterior notochord, revealed that the node does not regress posteriorly, and the cells in the node form trunk notochord by convergent-extension movements (Yamanaka et al., 2007). In contrast, the *Noto*-positive cells located at the peripheral node actively migrate toward the posterior, and probably generate the posterior extension of the notochord (Yamanaka et al., 2007). However, because live imaging is restricted to a single day of observation, it was unresolved whether these *Noto*-expressing cells actually contributed subsequently to the NPCs of the tail bud and generated the posterior extension of the notochord.

To address this issue, we performed lineage tracing of *Noto*-positive cells by genetically labeling the cells. For this purpose, we generated $Noto^{nmCherry\text{-}CreERT2}$ mice, which express tamoxifen-inducible Cre recombinase ($CreER^{T2}$) (Feil et al., 1997) from the *Noto* locus, with homologous recombination in ES cells. In this knock-in line, the coding sequences for nuclear fluorescent protein (*Histone H2B-mCherry*) (Shaner et al., 2005) and $CreER^{T2}$ were placed downstream of the *Noto* coding sequence, with sequences for virus-derived 2A peptides (Szymczak et al., 2004) inserted between the protein coding sequences (Fig. 2A, B). Because 2A peptide-containing proteins are self-cleaved downstream of the 2A peptide, their introduction allows the production of multiple, in this case three, proteins from a single transcript (Szymczak and Vignali, 2005; Szymczak et al., 2004) (Fig. 2A). We confirmed the successful homologous recombination between the *Noto* loci and deletion of the neomycin-

resistance gene cassette (ACN cassette) (Bunting et al., 1999) by Southern blotting and PCR (Fig. 2C-F).

The *Noto*$^{nmCherry\text{-}CreERT2}$ mouse lines were produced from three independent ES cell lines (#58, #62, #74). Because all three knock-in lines exhibited the same phenotype, we used the line derived from ES #62 for most of the analyses. Although we designed the mice to express Noto, approximately half of the *Noto*$^{nmCherry\text{-}CreERT2/nmCherry\text{-}CreERT2}$ mice showed various degrees of tail defects (curled, short, or no tail, data not shown), which resembled those of *Noto*$^{eGFP/eGFP}$ or *Noto*$^{tc/tc}$ mutant mice (Abdelkhalek et al., 2004). Therefore, it is likely that the addition of the 2A peptide to the Noto C-terminus interfered with the activity of the protein, or alternatively, the cleavage of the 2A sequence between Noto and the nuclear mCherry was incomplete.

Consistent with the expression of *Noto* in the ventral node and posterior notochord between E7.5 and E12.5 (Abdelkhalek et al., 2004; Plouhinec et al., 2004), the mCherry fluorescence was observed in the nuclei of the node and posterior notochord cells between E7.5 and E8.5 (arrowheads in Fig. 3A, A', B, B'). A faint mCherry signal was also observed in the tail bud in a notochord-like pattern at later stages (arrowheads in Figure 3C, C' and data not shown). The immunostaining of sections of E9.5 tail for mCherry confirmed the localization of the mCherry protein to the nuclei of notochord cells. Weaker signals were also observed in some of the paraxial mesoderm cells adjacent to the notochord. A similar paraxial expression of EGFP was also reported with *Noto*$^{eGFP/+}$ embryos (Yamanaka et al., 2007).

When Cre activity was induced by the oral administration of tamoxifen (Tx) to pregnant female mice at E8.5, the posterior notochord cells of *Noto*$^{nmCherry\text{-}CreERT2/+}$;*ROSA26*$^{LacZ/+}$ embryos were β-galactosidase-positive at E9.5 (Fig. 3D). In contrast, no labeled cells were observed without induction by Tx (Fig. 3E), suggesting that the self-cleavage at the 2A peptide between nuclear mCherry and CreER^{T2} took place efficiently. Tx administration at E7.75 led to dense labeling of the ventral node and sparse labeling of the posterior notochord at E8.5 (Fig. 3F). At E9.5, the labeling was present in a wide range of posterior notochord cells, including cells at the posterior end of the tail bud (Fig. 3G, H), indicating a broad distribution of NPCs. Because not all the ventral node cells were labeled with this protocol, the distribution of labeled cells in the notochord often appeared discontinuous. Similar labeling of the NPCs and posterior notochord was observed in E12.5 and E13.5 embryos (Fig. 3I and data not shown), but a scattered and segmental distribution of labeled cells in the non-notochordal mesoderm gradually became evident as development proceeded (asterisks in Fig. 3G, I, L). The contribution of Noto-positive cells to non-notochordal mesoderm is consistent with a previous observation that a minor population of eGFP-positive cells contributes to the non-notochordal mesoderm in *Noto*$^{eGFP/+}$ embryos (Yamanaka et al., 2007).

Finally, to restrict the Cre induction period to early stages, we also examined the effect of Tx administration at E6.5, when *Noto* is expressed in the anterior primitive streak (Plouhinec et al., 2004), the location of the presumptive NPCs (Kinder et al., 2001). At E7.5, dense labeling was observed in the ventral node, and sparse labeling in the anterior midline (Fig. 3J). At E10.5, strong labeling was observed in the posterior notochord (Fig. 3K, L), which was essentially the same pattern as obtained when Tx was administered at E7.75. Taken together, these results are consistent with the hypothesis that the NPCs of the tail bud originate from the *Noto*-positive cells of E7.5 to E8.5 embryos, which are probably the peripheral node cells that migrate toward the posterior, and that these cells generate the posterior extension of the notochord.

2.3. Active Wnt signaling co-localizes with NPCs

To address the mechanism by which the Noto-positive cells generate the posterior notochord extension in the tail bud, we focused on the Wnt signal, because mouse mutants of various Wnt

signaling components (Galceran et al., 1999; Kelly et al., 2004; Takada et al., 1994) lack a posterior trunk, but the role of Wnt signaling in posterior notochordal development has not been established. Because our previous study on *Foxa2*, an essential gene for node/notochord development, suggested that the control of NPC gene expression is downstream of Wnt signaling (Sawada et al., 2005), we first examined whether Wnt signaling was active in the NPCs. In an extension of previous studies that showed active Wnt signaling in the E7.5-8.5 node by using the transgenic Wnt reporter lines *BAT-gal*, *BATlacZ*, and *TOPGAL* (Maretto et al., 2003; Merrill et al., 2004; Nakaya et al., 2005), we investigated Wnt signaling in the NPCs after E8.5. Expression of the Wnt reporter gene *TOPGAL* in transgenic embryos was studied from E8.5 to E13.5. Strong TOPGAL expression was observed in the ventral layer of the E8.5 node, confirming previous reports (Fig. 4A). Strong TOPGAL activity was also detected in the posterior notochordal region, with a decrease in activity in the anterior notochord at E8.75 and E9.5 (Fig. 4B, 5G). Thus, robust Wnt signaling is active in the tissue area where NPCs reside.

Since the posterior extension of the tail continues until E13, NPCs are presumably maintained until this stage. Until E12.5, TOPGAL expression patterns similar to those at E9.5 were observed in the tail region, but TOPGAL began to decrease at E12.5 (Fig. 4C, D) and was barely detectable by E13.5 (Figure 4E). Therefore, TOPGAL expression coincided with the expected localization of the NPCs.

To corroborate our findings on TOPGAL expression, we used a second transgenic Wnt reporter line, *ins-TOPGAL* (Moriyama et al., 2007), in which the transgene is flanked by the core element of the chicken *β-globin* HS4 insulator (Recillas-Targa et al., 2002) to eliminate the effects of surrounding genes. The *ins-TOPGAL* generally leads to a stronger and broader expression of β-galactosidase than *TOPGAL*. Although *ins-TOPGAL* was expressed in all the tissues in the posterior embryo around E9.5 (Fig. 4G), the faster development of the reaction product in the posterior notochord clearly indicated that its expression was much stronger in the posterior notochord than in the surrounding tissues (Fig. 4H, I). Taken together, these data indicate that Wnt signaling is strongly active in the NPCs.

2.4. Notochord-specific gene ablation of β-catenin

To clarify the role of Wnt signaling in the NPCs, we conditionally inactivated the *β-catenin* gene by the combined use of floxed *β-catenin* (Brault et al., 2001) and a second notochord-specific Cre transgene, *Not-Cre*. The *Not-Cre* mouse is an enhancer trap line (see Experimental Procedures). We used this constitutive Cre line for the complete deletion of *β-catenin*, because the deletion by induced Cre with $Noto^{nmCherry\text{-}CreERT2/+}$ was much less effective, and the resulting mutant embryos showed no apparent abnormalities (data not shown). The *Not-Cre* transgenic embryos exhibited detectable Cre activity in notochord from E8.25, and after E8.5, its strong activity prevailed the entire notochord (Fig. 5A-D). In normal embryo at E9.25, β-catenin protein strongly accumulated in the notochord, while $Not\text{-}Cre;\beta\text{-}catenin^{flox/flox}$ embryos showed notchord-specific reduction of β-catenin accumulation (Fig. 5E, F). Consistently, in $Not\text{-}Cre;\beta\text{-}catenin^{flox/flox}$ embryos, *TOPGAL* expression in the posterior notochord was clearly reduced after E9.25, which followed *β-catenin* ablation (Fig. 5G-J). The significantly weaker β-galactosidase signals in these sections clearly indicated reduced *TOPGAL* expression in individual notochord cells (Fig. 5I, J). Thus, in $Not\text{-}Cre;\beta\text{-}catenin^{flox/flox}$ embryos, Wnt signaling in the NPCs was reduced after E9.25, and this was utilized in the further analyses.

2.5. Attenuation of posterior notochord development via β-catenin ablation

The gross morphology of embryos was not significantly altered after notochordal *β-catenin* ablation at E9.5, but histological analysis indicated that the posterior notochord was smaller

(Fig. 5G-J, 6A, B). At E10.5, *β-catenin*-ablated embryos showed a bent and shortened tail that lacked a notochord (Figures 6C-F). These embryos developed to term and survived at least to weaning age. However, they lacked a tail and their posterior vertebrae were truncated at the lumbar region (L6) or the first sacral vertebra (S1) (Fig. 6G, H and data not shown). These results indicate that Wnt signaling in the NPCs is required for the posterior extension of the notochord and for the complete development of the tail.

2.6. Altered gene expression profile at the notochord posterior end

We examined whether the identity of NPCs was still maintained if Wnt signaling was inhibited. *Noto* is expressed specifically in the posterior end of the notochord (Abdelkhalek et al., 2004; Plouhinec et al., 2004), and *Noto* expression was dramatically reduced in the *Not-Cre;β-catenin*$^{flox/flox}$ mutants (Fig. 7A, B). However, notochord-like tissue was still morphologically identifiable on sections in the absence of *Noto* expression (Fig. 7C, D, n = 8/8). When notochordal *β-catenin* was ablated, *Brachyury* expression in the posterior notochord (Wilkinson et al., 1990) was clearly reduced without significantly affecting its expression in the anterior notochord (Fig. 7E-J, n = 6/6). Similarly, the expression of *Sonic hedgehog (Shh)* was dramatically reduced, but again only in the posterior notochord (Echelard et al., 1993) (Fig. 7K, L and data not shown, n = 5/5).

We further investigated the nature of the notochord-like tissue that formed in the posterior region even in the absence of *Noto, Brachyury*, or *Shh*. Interestingly, *Foxa1* and *Foxa2*, which are expressed in both the notochord and the endoderm (Sasaki and Hogan, 1993), were expressed in the mutant embryos at normal levels (Fig. 7M-P, n = 5/5 and n = 5/5, respectively). We therefore examined the possibility that the NPCs' fate had been re-specified to an endodermal one. Indeed, notochord-specific *β-catenin* ablation resulted in the ectopic expression of E-cadherin, which is expressed in the endoderm but not in the notochord (Nose and Takeichi, 1986), in the posterior notochord at E9.5 (Fig. 7Q, Q', R, R', n = 7/7). The frequent accumulation of E-cadherin at cell-cell boundaries in the mutant notochord (data not shown) suggests that cadherin-mediated cell adhesion was maintained in the *β-catenin*-ablated cells, probably owing to the presence of plakoglobin and/or residual β-catenin. However, we failed to observe an increased expression of other endoderm-specific genes, *Rbm35* or *Ripk4* (Sherwood et al., 2007) (data not shown). These observations suggest that Wnt/β-catenin signaling is required to maintain the notochordal identity of the NPCs, and under reduced Wnt/β-catenin signaling, the expression of notochord-specific genes is lost and only the genes expressed in both the notochord and the endoderm are maintained.

2.7. No significant alteration in cell proliferation or apoptosis

Because Wnt signaling often acts as a mitogen in progenitor cells, we next asked whether cell proliferation and survival of the *β-catenin*-ablated posterior notochord/NPCs was altered, by BrdU labeling and TUNEL staining, at E9.25. Although the total cell number was already reduced in the *β-catenin*-ablated posterior notochord, the fraction of BrdU-positive cells was comparable to that in normal notochord, indicating that cell proliferation was not significantly affected (Fig. 7S, T, W). Similarly, TUNEL analysis showed similar levels of apoptosis between the wild-type and mutant NPCs (Fig. 7, U, V, X). Taken together, these results indicate that Wnt signaling is required only for the cell-fate specification of NPCs and that it is dispensable for their proliferation.

3. Discussion

3.1 Origin of the NPCs in the tail bud

We have shown with genetic cell labeling that the *Noto*-expressing ventral node cells contribute the NPCs that generate the entire posterior notochord, including the posterior end, and therefore

also contribute the NPCs of the tail bud. Consistent with this observation, previous dye labeling and transplantation experiments showed that NPCs reside in the ventral node, especially in the boundary region between the node and the primitive streak (Beddington, 1994; Cambray and Wilson, 2002; Cambray and Wilson, 2007; Wilson and Beddington, 1996). Noto-expressing cells from this region or the periphery of the node actively migrate toward the posterior (Yamanaka et al., 2007). Taken together, our results are consistent with the hypothesis that *Noto*-expressing and posteriorly migrating cells from around the node constitute the NPCs in the tail bud, and these cells generate the posterior extension of the notochord.

3.2 Wnt signaling maintains the notochordal fate of NPCs

NPCs in both the ventral node and the tail bud express notochord-specific genes (Gofflot et al., 1997), and when transplanted to ectopic sites, the node produces an ectopic notochord (Beddington, 1994; Kinder et al., 2001). Therefore, NPCs have been considered to be committed to the notochordal fate. In this study, however, we demonstrated that the notochordal identity of NPCs depends on a sustained supply of Wnt signaling. In its absence, the NPCs lost their expression of notochord-specific genes, and they maintained only the expression of genes that were expressed in both the notochord and the endoderm. Assuming that the NPCs in the node originally derive from mesoendodermal cells located at the anterior end of the primitive streak of the gastrula, and that this process requires Wnt signaling (Lickert et al., 2002), it is likely that NPCs in the node and tail bud remain in a transitional state of differentiation from the mesoendoderm to the notochord, despite their earlier expression of notochord-specific genes. Therefore, NPCs are partially committed cells, and the role of Wnt signaling is to maintain their notochordal fate. In this paper, we used the constitutive Cre line, *Not-Cre*, for the complete deletion of *β-catenin*, because deletion by induced Cre with $Noto^{nmCherry\text{-}CreERT2/+}$ was much less effective. Since *Not-Cre* transgenic mouse also showed weaker Cre activity in the posterior endoderm and mesoderm (Fig. 5C,D), we cannot officially rule out the possibility that presence of *β-catenin*—ablated cells in the non-notochordal tissues caused the observed notochordal defects; however, we did not find non-notochordal cells showing reduced β-catenin levels by immunostaining (Fig. 5F).

Wnt signaling plays a similar role in fate specification in other stem/progenitor cell systems, including in skin development (Reya and Clevers, 2005). Although Wnt signaling is mitogenic in other systems (for example, in hematopoietic stem cells (Willert et al., 2003)), we did not observe significant changes in cell proliferation in the *β-catenin*-ablated NPCs. Therefore, the exact mechanism for the loss of posterior notochord in these mutants is currently unknown. Some other signaling pathway, however, might be responsible for stimulating the NPCs to proliferate. For example, in the zebrafish tailbud, Bmp4 signaling promotes cell proliferation and inhibits maturation of the notochord (Esterberg et al., 2008). It is tempting to speculate that Bmp signaling plays similar mitogenic roles in mouse NPCs, and that Wnt and Bmp signaling cooperatively regulate notochord development.

The role of Wnt signaling in the maintenance of NPC identity is likely to be evolutionally conserved. In support of this assertion, a similar activation of Wnt signaling at the posterior end of developing *Xenopus* was observed to follow β-catenin accumulation in the nucleus (Schohl and Fagotto, 2002). Likewise, *Wnt3a* knockdown in zebrafish embryos results in posterior notochord truncation in the tail (Thorpe et al., 2005). Because of these similarities, we believe that the abnormalities observed in our current study are primarily attributable to the attenuation of Wnt signaling. Nonetheless, the involvement of other effects caused by the reduced β-catenin levels cannot be formally excluded. Moreover, given that the notochordal truncation phenotypes in this mouse *β-catenin* ablation model and the zebrafish *Wnt3a* knockdown (Thorpe et al., 2005) are similar, and given the posterior body truncation seen in *Wnt3a* mouse mutants (Takada et al., 1994), Wnt3a is a logical candidate for the ligand that

acts on the NPCs. In further support of this idea, the timing of the gradual decrease of Wnt3a expression during elongation arrest of the mouse tail (Cambray and Wilson, 2007) matches the gradual reduction of TOPGAL in the NPCs. Although Wnt8 plays a synergistic role in zebrafish tail development (Shimizu et al., 2005; Thorpe et al., 2005), the E9.5 mouse tail bud expresses neither Wnt8a nor Wnt8b (K.U. and H.S., unpublished observation).

4. Experimental procedures

4.1. Mouse lines

The *Noto*$^{nmCherry\text{-}CreERT2/+}$ (Acc. No. CDB0579K: http://www.cdb.riken.jp/arg/mutant%20mice%20list.html) mouse was generated by homologous recombination in ES cells as follows. The C57BL/6 mouse BAC genomic DNA clone RP23-437M22, which contains the *Noto* gene, was obtained from BACPAC Resources, Children's Hospital Oakland Research Institute, and the gene with its surrounding genomic material was subcloned into MC1-DTA-pA/pMW118 (Nishioka et al., 2008; Sawada et al., 2008) using homologous recombination in E. coli, a recombineering method (Liu et al., 2003).

The *Noto* targeting vector was designed to remove the termination codon of the Noto protein, and introduced upstream of the following sequences: Equine rhinitis A virus (ERAV) 2A peptide (Szymczak and Vignali, 2005), a fusion protein of human histone H2B and mCherry (Shaner et al., 2005), *Thosea asigna* virus (TaV) 2A peptide (Szymczak and Vignali, 2005), and CreER^{T2} (Feil et al., 1997). The neomycin-resistance gene was supplied as the ACN cassette, which is self-excised in the germ line (Bunting et al., 1999). The targeting vector was generated using a recombineering method (Liu et al., 2003).

TT-2 ES cells (Yagi et al., 1993) were transformed by electroporation with the linearized targeting vector, followed by positive and negative selection with G418 and DT-A, respectively (Murata et al., 2004). The ES clones were screened for homologous recombination by long polymerase chain reaction (PCR) using LA-Taq (TaKaRa, Japan), as described (Murata et al., 2004). To screen for the *Noto* locus, the following primer pair was used: SVloxP-3′-F2 (AGGCCCAGGGCTCGCAGCCAACGTCG) and Noto-PC-3′-R2 (TTCAGGAGGTGAGGGCAGGGAGGACC). The positions of these primers are indicated in Fig. 2A. Correct homologous recombination of the *Noto* locus and the absence of randomly inserted targeting vectors were confirmed in the PCR-positive clones by Southern hybridization (Fig. 2B-D). The confirmed ES clones were injected into 8-cell embryos to produce chimeric mice. Chimeric founders from three independent ES cell lines (#58, #62, #74) were crossed with C57BL/6 mice, and the resulting knock-in mouse lines were maintained on the C57BL/6 background. Confirmation that the ACN cassette had been removed and genotype determination were performed by PCR with primers that produced both knock-in and wild-type bands: *Noto* genotype F (nF, GTGCGGTGACTGAGAGCTTAGG), *Noto* genotype R (nR, CGTCTATCCCATAAACCTCACC), *ERT2* genotype F (eF, GGGCTCTACTTCATCGCATTCC). The positions of these primers are indicated in Fig. 2A. A 545-bp product is generated from the wild-type allele of nF and nR, and a 389-bp product is generated from the knock-in allele with eF and nR. The PCR conditions were 95 °C for 1 min, 30 cycles of 95 °C for 30 seconds, 58 °C for 30 seconds, 72 °C for 1 min, followed by 72 °C for 5 min. To induce Cre activity, pregnant mice were given tamoxifen (Sigma, T5648) dissolved in peanut oil (10 mg/ml) at 0.12 mg/g body weight, by oral gavage, as described previously (Park et al., 2008).

The floxed *β-catenin* mutant (Brault et al., 2001), *TOPGAL* (Merrill et al., 2004), and *ROSA26R* (Soriano, 1999) mice were all obtained from The Jackson Laboratory. The *Not-Cre* mouse line was incidentally established while generating a Pax6(Lens)-Cre transgenic

mouse (Yoshimoto et al., 2005). The transgene integration site was assigned to Chr 5, C1 by chromosomal FISH. The *ins-TOPGAL* line was described elsewhere (Moriyama et al., 2007). Mice were housed in environmentally controlled rooms of the Laboratory Animal Housing Facility of RIKEN Center for Developmental Biology, under the institutional guidelines for animal and recombinant DNA experiments.

4.2. Preparation of skeletal specimens

The cartilage and bone from P0 neonates and weaning-age (four weeks) mice were stained with Alucian Blue and Alizarin Red, respectively, as described (Hogan et al., 1994).

4.3. In situ hybridization

Whole-mount *in situ* hybridization and the sectioning of stained embryos were performed as described (Sasaki and Hogan, 1993). Probes for *Not* (Abdelkhalek et al., 2004) and *Foxa1* were described previously (Sasaki and Hogan, 1993). Probes for *Brachyury* and *Shh* were gifts from Drs. S. Takada and H. Hamada, respectively.

4.4. Antibody staining

Immunohistochemical and immunofluorescence staining of paraffin sections from embryos were performed according to standard procedures. Briefly, sections were incubated with a rabbit anti-Foxa2 antibody (1:100) (Yasui et al., 1997), rabbit anti-β-catenin antibody (Sigma, 1:4000), or mouse anti-E-cadherin antibody (BD Biosciences, 1:250) at 4°C overnight, followed by detection with anti-rabbit IgG conjugated with alkaline phosphatase (Jackson ImmunoResearch Laboratories) or Alexa594 (Molecular Probes). Immunofluorescence staining for mCherry protein was performed on cryosections of embryos using an anti-DsRed antibody (Clontech, 1:500), followed by detection with anti-rabbit IgG-Alexa594 (Molecular Probes), and DAPI.

4.5. Analysis of cell proliferation and apoptosis

Proliferating cells were detected via BrdU-labeling by combining the described procedures (Liu et al., 2000; Megason and McMahon, 2002). Briefly, pregnant mice were given intra-peritoneal injections of BrdU at 200 μg/g body weight, 2 hours prior to dissection. The embryos were fixed with 4% paraformaldehyde (PFA) in phosphate-buffered saline (PBS), and paraffin sections were prepared. To detect BrdU incorporation, deparaffinized and rinsed sections were incubated in 200 ng/ml Proteinase K in PBS for 5 minutes at room temperature, rinsed, incubated in 50% formamide, 1x SSC, 0.1% Tween-20 at 65°C for 2 hours, in 2N-HCl for 15 minutes, and in 0.1 M $Na_2B_4O_7$ (pH 8.5) for 10 min, rinsed again, and stained with mouse monoclonal anti-BrdU (Sigma, 1:1000), anti-mouse IgG-Alexa594, and DAPI. Apoptosis was detected using the ApopTag Red In Situ Apoptosis Detection Kit (Chemicon) following the manufacturer's instructions. The numbers of notochord cells and of labeled notochord cells within 100 μm of the posterior end of the notochord (E9.25 and E10.5) or the ventral node (E7.75) were counted on two (E9.25), three (E10.5), or five (E7.75) sections per embryo, and the total numbers were used for statistical analyses. Statistical analyses were performed with Prism5 statistical software (GraphPad) using an unpaired, two-tailed *t*-test.

4.6 β-galactosidase staining of embryos

Whole-mount staining of embryos for β-galactosidase activity, and paraffin sectioning of the stained embryos were performed as described (Wurst and Gossler, 2000).

4.7 Imaging

Images of the whole-mount embryos and sections were acquired with a Leica MZ16 or Axioplan2 (Zeiss) microscope equipped with an AxioCam HRc (Zeiss) or AxioCamMRm (Zeiss). For some images of whole-mount embryos, all-focal-levels images were generated by merging multiple images of different focal planes using Dynamic Eye REAL software (Mitani Corporation, Japan). Confocal images of whole-mount embryos were acquired with a Nikon AZ-C1 macro-confocal microscope.

Acknowledgments

We thank Ms. M. Shibata for mouse genotyping; Ms. M. Harano for technical assistance; the Laboratory for Animal Resources and Genetic Engineering for generating the mutant mice and housing all the mice; Dr. I. Matsuo for sharing mice; Dr. M. Seiki-Furutani for sharing unpublished information; Dr. Y. Saijoh for advice on Cre induction by Tamoxifen administration; Dr. H. Enomoto for advice on knock-in strategy and plasmids; Dr. N. Copeland for the recombineering system; Dr. K.R. Thomas for ACN cassette plasmid; Dr. P. Chambon for CreER^{T2} plasmid; and Drs. S. Takada, A. Gossler, H. Hamada, and R. I. Sherwood for *in situ* probes. This work was supported by a grant from RIKEN to HS, National Institutes of Health grant NICHD to R. R. B., and Grants-in-Aid for Scientific Research 17107005 to HK from the Ministry of Education, Culture, Sports, Science and Technology of Japan.

References

Abdelkhalek HB, Beckers A, Schuster-Gossler K, Pavlova MN, Burkhardt H, Lickert H, Rossant J, Reinhardt R, Schalkwyk LC, Muller I, Herrmann BG, Ceolin M, Rivera-Pomar R, Gossler A. The mouse homeobox gene Not is required for caudal notochord development and affected by the truncate mutation. Genes Dev 2004;18:1725–36. [PubMed: 15231714]

Agathon A, Thisse C, Thisse B. The molecular nature of the zebrafish tail organizer. Nature 2003;424:448–52. [PubMed: 12879074]

Ang SL, Rossant J. HNF-3 β is essential for node and notochord formation in mouse development. Cell 1994;78:561–574. [PubMed: 8069909]

Beck CW, Slack JM. A developmental pathway controlling outgrowth of the Xenopus tail bud. Development 1999;126:1611–20. [PubMed: 10079224]

Beck CW, Whitman M, Slack JM. The role of BMP signaling in outgrowth and patterning of the Xenopus tail bud. Dev Biol 2001;238:303–14. [PubMed: 11784012]

Beddington RS. Induction of a second neural axis by the mouse node. Development 1994;120:613–20. [PubMed: 8162859]

Bellomo D, Lander A, Harragan I, Brown NA. Cell proliferation in mammalian gastrulation: the ventral node and notochord are relatively quiescent. Dev Dyn 1996;205:471–85. [PubMed: 8901057]

Brault V, Moore R, Kutsch S, Ishibashi M, Rowitch DH, McMahon AP, Sommer L, Boussadia O, Kemler R. Inactivation of the beta-catenin gene by Wnt1-Cre-mediated deletion results in dramatic brain malformation and failure of craniofacial development. Development 2001;128:1253–64. [PubMed: 11262227]

Bunting M, Bernstein KE, Greer JM, Capecchi MR, Thomas KR. Targeting genes for self-excision in the germ line. Genes Dev 1999;13:1524–8. [PubMed: 10385621]

Cambray N, Wilson V. Axial progenitors with extensive potency are localised to the mouse chordoneural hinge. Development 2002;129:4855–66. [PubMed: 12361976]

Cambray N, Wilson V. Two distinct sources for a population of maturing axial progenitors. Development 2007;134:2829–40. [PubMed: 17611225]

Cleaver O, Krieg PA. Notochord patterning of the endoderm. Dev Biol 2001;234:1–12. [PubMed: 11356015]

Davidson BP, Tam PP. The node of the mouse embryo. Curr Biol 2000;10:R617–9. [PubMed: 10996084]

Echelard Y, Epstein DJ, St-Jacques B, Shen L, Mohler J, McMahon JA, McMahon AP. Sonic hedgehog, a member of a family of putative signaling molecules, is implicated in the regulation of CNS polarity. Cell 1993;75:1417–30. [PubMed: 7916661]

Esterberg R, Delalande JM, Fritz A. Tailbud-derived Bmp4 drives proliferation and inhibits maturation of zebrafish chordamesoderm. Development 2008;135:3891–901. [PubMed: 18948415]

Feil R, Wagner J, Metzger D, Chambon P. Regulation of Cre recombinase activity by mutated estrogen receptor ligand-binding domains. Biochem Biophys Res Commun 1997;237:752–7. [PubMed: 9299439]

Galceran J, Farinas I, Depew MJ, Clevers H, Grosschedl R. Wnt3a-/--like phenotype and limb deficiency in Lef1(-/-)Tcf1(-/-) mice. Genes Dev 1999;13:709–17. [PubMed: 10090727]

Gofflot F, Hall M, Morriss-Kay GM. Genetic patterning of the developing mouse tail at the time of posterior neuropore closure. Dev Dyn 1997;210:431–45. [PubMed: 9415428]

Gont LK, Steinbeisser H, Blumberg B, de Robertis EM. Tail formation as a continuation of gastrulation: the multiple cell populations of the Xenopus tailbud derive from the late blastopore lip. Development 1993;119:991–1004. [PubMed: 7916680]

Griffith CM, Wiley MJ, Sanders EJ. The vertebrate tail bud: three germ layers from one tissue. Anat Embryol (Berl) 1992;185:101–13. [PubMed: 1536443]

Herrmann BG, Kispert A. The T genes in embryogenesis. Trends Genet 1994;10:280–6. [PubMed: 7940757]

Hogan, B.; Beddington, R.; Constantini, F.; Lacy, E. Manipulating the Mouse Embryo: Laboratory Manual. Vol. 2nd edn.. Cold Spring Harbor Laboratory Press; 1994.

Kelly OG, Pinson KI, Skarnes WC. The Wnt co-receptors Lrp5 and Lrp6 are essential for gastrulation in mice. Development 2004;131:2803–15. [PubMed: 15142971]

Kinder SJ, Tsang TE, Wakamiya M, Sasaki H, Behringer RR, Nagy A, Tam PP. The organizer of the mouse gastrula is composed of a dynamic population of progenitor cells for the axial mesoderm. Development 2001;128:3623–34. [PubMed: 11566865]

Lickert H, Kutsch S, Kanzler B, Tamai Y, Taketo MM, Kemler R. Formation of multiple hearts in mice following deletion of beta-catenin in the embryonic endoderm. Dev Cell 2002;3:171–81. [PubMed: 12194849]

Liu P, Jenkins NA, Copeland NG. A highly efficient recombineering-based method for generating conditional knockout mutations. Genome Res 2003;13:476–84. [PubMed: 12618378]

Liu, Y-H.; Snead, ML.; Maxon, RE, Jr.. Transgenic mouse models of craniofacial disorders. In: Tuan, RS., editor. Methods Mol. Biol, Vol 137: Developmental Biology Protocols. Vol. III. Vol. 137. Humana Press Inc; NJ: 2000. p. 499-511.

Maretto S, Cordenonsi M, Dupont S, Braghetta P, Broccoli V, Hassan AB, Volpin D, Bressan GM, Piccolo S. Mapping Wnt/beta-catenin signaling during mouse development and in colorectal tumors. Proc Natl Acad Sci U S A 2003;100:3299–304. [PubMed: 12626757]

Megason SG, McMahon AP. A mitogen gradient of dorsal midline Wnts organizes growth in the CNS. Development 2002;129:2087–98. [PubMed: 11959819]

Merrill BJ, Pasolli HA, Polak L, Rendl M, Garcia-Garcia MJ, Anderson KV, Fuchs E. Tcf3: a transcriptional regulator of axis induction in the early embryo. Development 2004;131:263–74. [PubMed: 14668413]

Moriyama A, Kii I, Sunabori T, Kurihara S, Takayama I, Shimazaki M, Tanabe H, Oginuma M, Fukayama M, Matsuzaki Y, Saga Y, Kudo A. GFP transgenic mice reveal active canonical Wnt signal in neonatal brain and in adult liver and spleen. Genesis 2007;45:90–100. [PubMed: 17245775]

Murata T, Furushima K, Hirano M, Kiyonari H, Nakamura M, Suda Y, Aizawa S. ang is a novel gene expressed in early neuroectoderm, but its null mutant exhibits no obvious phenotype. Gene Expr Patterns 2004;5:171–8. [PubMed: 15567712]

Nakaya MA, Biris K, Tsukiyama T, Jaime S, Rawls JA, Yamaguchi TP. Wnt3alinks left-right determination with segmentation and anteroposterior axis elongation. Development 2005;132:5425–36. [PubMed: 16291790]

Niehrs C. Regionally specific induction by the Spemann-Mangold organizer. Nat Rev Genet 2004;5:425–34. [PubMed: 15153995]

Nishioka N, Yamamoto S, Kiyonari H, Sato H, Sawada A, Ota M, Nakao K, Sasaki H. Tead4 is required for specification of trophectoderm in pre-implantation mouse embryos. Mech Dev 2008;125:270–83. [PubMed: 18083014]

Nishizaki Y, Shimazu K, Kondoh H, Sasaki H. Identification of essential sequence motifs in the node/notochord enhancer of Foxa2 (Hnf3β) gene that are conserved across vertebrate species. Mech Dev 2001;102:57–66. [PubMed: 11287181]

Nose A, Takeichi M. A novel cadherin cell adhesion molecule: its expression patterns associated with implantation and organogenesis of mouse embryos. J Cell Biol 1986;103:2649–58. [PubMed: 3539943]

Park EJ, Sun X, Nichol P, Saijoh Y, Martin JF, Moon AM. System for tamoxifen-inducible expression of cre-recombinase from the Foxa2 locus in mice. Dev Dyn 2008;237:447–53. [PubMed: 18161057]

Plouhinec JL, Granier C, Le Mentec C, Lawson KA, Saberan-Djoneidi D, Aghion J, Shi DL, Collignon J, Mazan S. Identification of the mammalian Not gene via a phylogenomic approach. Gene Expr Patterns 2004;5:11–22. [PubMed: 15533813]

Recillas-Targa F, Pikaart MJ, Burgess-Beusse B, Bell AC, Litt MD, West AG, Gaszner M, Felsenfeld G. Position-effect protection and enhancer blocking by the chicken beta-globin insulator are separable activities. Proc Natl Acad Sci U S A 2002;99:6883–8. [PubMed: 12011446]

Reya T, Clevers H. Wnt signalling in stem cells and cancer. Nature 2005;434:843–50. [PubMed: 15829953]

Sasaki H, Hogan BL. Differential expression of multiple fork head related genes during gastrulation and axial pattern formation in the mouse embryo. Development 1993;118:47–59. [PubMed: 8375339]

Sasaki H, Hogan BL. Enhancer analysis of the mouse HNF-3β gene: regulatory elements for node/notochord and floor plate are independent and consist of multiple sub-elements. Genes Cells 1996;1:59–72. [PubMed: 9078367]

Sawada A, Kiyonari H, Ukita K, Nishioka N, Imuta Y, Sasaki H. Redundant roles of Tead1 and Tead2 in notochord development and the regulation of cell proliferation and survival. Mol Cell Biol 2008;28:3177–89. [PubMed: 18332127]

Sawada A, Nishizaki Y, Sato H, Yada Y, Nakayama R, Yamamoto S, Nishioka N, Kondoh H, Sasaki H. Tead proteins activate the Foxa2 enhancer in the node in cooperation with a second factor. Development 2005;132:4719–29. [PubMed: 16207754]

Schohl A, Fagotto F. Beta-catenin, MAPK and Smad signaling during early Xenopus development. Development 2002;129:37–52. [PubMed: 11782399]

Shaner NC, Steinbach PA, Tsien RY. A guide to choosing fluorescent proteins. Nat Methods 2005;2:905–9. [PubMed: 16299475]

Sherwood RI, Jitianu C, Cleaver O, Shaywitz DA, Lamenzo JO, Chen AE, Golub TR, Melton DA. Prospective isolation and global gene expression analysis of definitive and visceral endoderm. Dev Biol 2007;304:541–55. [PubMed: 17328885]

Shimizu T, Bae YK, Muraoka O, Hibi M. Interaction of Wnt and caudal-related genes in zebrafish posterior body formation. Dev Biol 2005;279:125–41. [PubMed: 15708563]

Soriano P. Generalized lacZ expression with the ROSA26 Cre reporter strain. Nat Genet 1999;21:70–1. [PubMed: 9916792]

Szymczak AL, Vignali DA. Development of 2A peptide-based strategies in the design of multicistronic vectors. Expert Opin Biol Ther 2005;5:627–38. [PubMed: 15934839]

Szymczak AL, Workman CJ, Wang Y, Vignali KM, Dilioglou S, Vanin EF, Vignali DA. Correction of multi-gene deficiency in vivo using a single ‘self-cleaving’ 2A peptide-based retroviral vector. Nat Biotechnol 2004;22:589–94. [PubMed: 15064769]

Takada S, Stark KL, Shea MJ, Vassileva G, McMahon JA, McMahon AP. Wnt-3a regulates somite and tailbud formation in the mouse embryo. Genes Dev 1994;8:174–89. [PubMed: 8299937]

Tam PP, Behringer RR. Mouse gastrulation: the formation of a mammalian body plan. Mech Dev 1997;68:3–25. [PubMed: 9431800]

Tam PP, Steiner KA, Zhou SX, Quinlan GA. Lineage and functional analyses of the mouse organizer. Cold Spring Harb Symp Quant Biol 1997;62:135–44. [PubMed: 9598345]

Thorpe CJ, Weidinger G, Moon RT. Wnt/beta-catenin regulation of the Sp1-related transcription factor sp5l promotes tail development in zebrafish. Development 2005;132:1763–72. [PubMed: 15772132]

Vincent SD, Dunn NR, Hayashi S, Norris DP, Robertson EJ. Cell fate decisions within the mouse organizer are governed by graded Nodal signals. Genes Dev 2003;17:1646–62. [PubMed: 12842913]

Weinstein DC, Ruiz i Altaba A, Chen WS, Hoodless P, Prezioso VR, Jessell TM, Darnell JE Jr. The winged-helix transcription factor HNF-3 β is required for notochord development in the mouse embryo. Cell 1994;78:575–88. [PubMed: 8069910]

Wilkinson DG, Bhatt S, Herrmann BG. Expression pattern of the mouse T gene and its role in mesoderm formation. Nature 1990;343:657–9. [PubMed: 1689462]

Willert K, Brown JD, Danenberg E, Duncan AW, Weissman IL, Reya T, Yates JR 3rd, Nusse R. Wnt proteins are lipid-modified and can act as stem cell growth factors. Nature 2003;423:448–52. [PubMed: 12717451]

Wilson V, Beddington RS. Cell fate and morphogenetic movement in the late mouse primitive streak. Mech Dev 1996;55:79–89. [PubMed: 8734501]

Wurst, W.; Gossler, A. Gene trap strategies in ES cells. In: Joyner, AL., editor. Gene Targeting. A Practical Approach. Oxford University Press Inc; New York: 2000.

Yagi T, Tokunaga T, Furuta Y, Nada S, Yoshida M, Tsukada T, Saga Y, Takeda N, Ikawa Y, Aizawa S. A novel ES cell line, TT2, with high germline-differentiating potency. Anal Biochem 1993;214:70–6. [PubMed: 8250257]

Yamamoto M, Meno C, Sakai Y, Shiratori H, Mochida K, Ikawa Y, Saijoh Y, Hamada H. The transcription factor FoxH1 (FAST) mediates Nodal signaling during anterior-posterior patterning and node formation in the mouse. Genes Dev 2001;15:1242–56. [PubMed: 11358868]

Yamanaka Y, Tamplin OJ, Beckers A, Gossler A, Rossant J. Live imaging and genetic analysis of mouse notochord formation reveals regional morphogenetic mechanisms. Dev Cell 2007;13:884–96. [PubMed: 18061569]

Yasui K, Sasaki H, Arakaki R, Uemura M. Distribution pattern of HNF-3beta proteins in developing embryos of two mammalian species, the house shrew and the mouse. Dev Growth Differ 1997;39:667–76. [PubMed: 9493826]

Yoshimoto A, Saigou Y, Higashi Y, Kondoh H. Regulation of ocular lens development by Smad-interacting protein 1 involving Foxe3 activation. Development 2005;132:4437–48. [PubMed: 16162653]

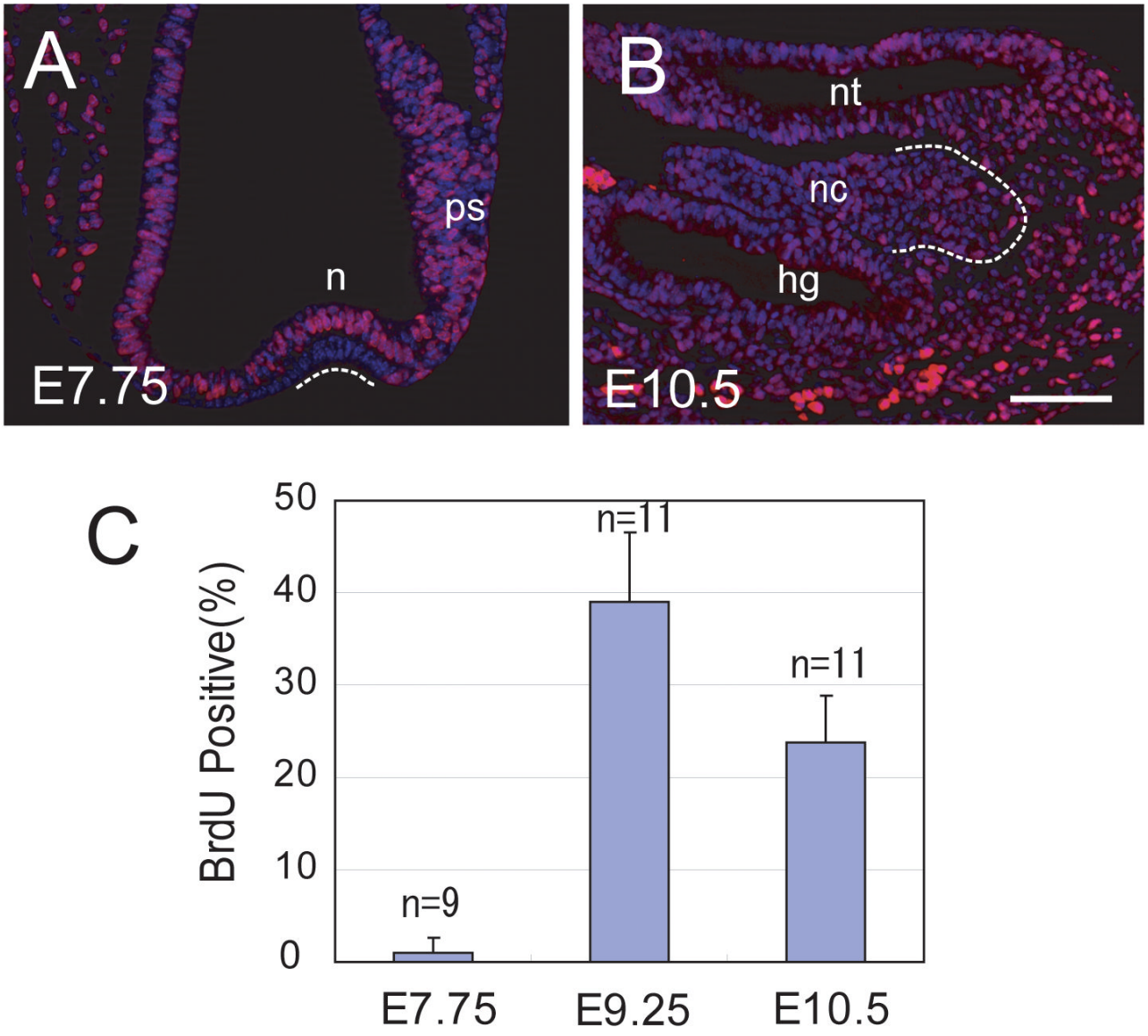

Figure 1. Proliferation of NPCs during development

(A, B) BrdU-labeling of (A) the E7.75 node (indicated by a dotted line) and (B) the E10.5 tail region of normal embryos. The posterior end of the notochord is surrounded by a dotted line. A representative E9.25 tail region is shown in Figure 5I. (C) Ratios of BrdU-positive cells in the node (E7.75) or at the posterior end of the notochord (E9.25 and E10.5).

Scale bar, 100 μm for A and B.

Abbreviations: hg, hindgut; n, node; nc, notochord; nt, neural tube; ps, primitive streak.

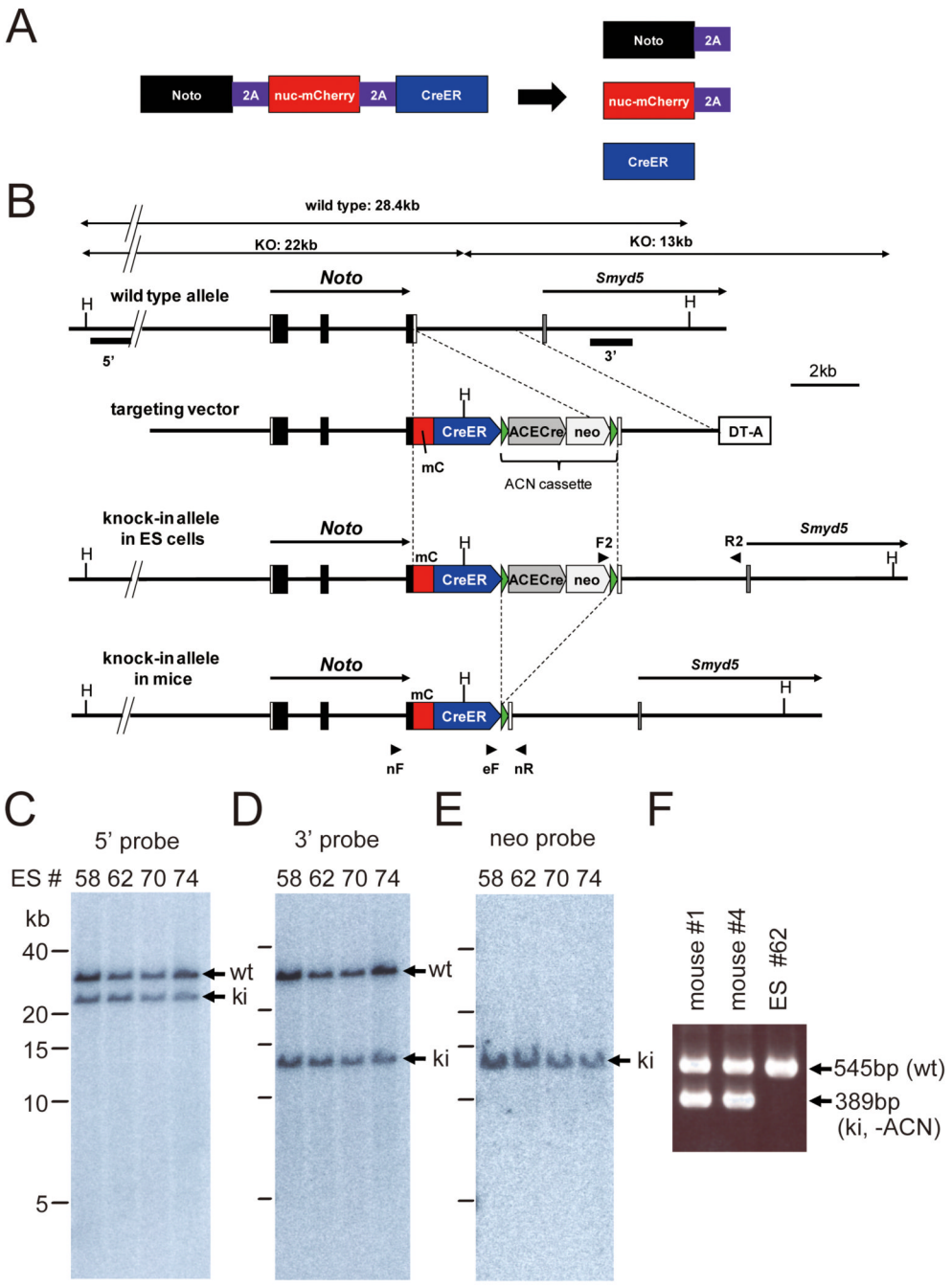

Figure 2. Production of the *Noto*$^{nmCherry\text{-}CreERT2/+}$ mouse

(A) Production of three proteins from a single transcript. 2A-peptide-containing proteins are self-cleaved downstream of the 2A peptide. Therefore, the modified *Noto*-locus, which has a single coding sequence for a Noto-2A-nuclear mCherry-2A-CreER^{T2} protein, will produce three proteins: Noto-2A, nuclear mCherry-2A, and CreER^{T2}.

(B) Targeting strategy. The *Noto*$^{nmCherry\text{-}CreERT2}$ allele was generated by homologous recombination in ES cells. Exons are indicated by filled and open boxes, and coding regions by filled boxes. Green triangles represent loxP sites. 5′ and 3′ indicate the approximate positions of probes for Southern hybridization. Abbreviations: H, Hind III; mC, ERAV 2A peptide followed by nuclear mCherry; CreER, TaV 2A peptide followed by CreER^{T2}; ACE-Cre, a

cassette carrying the testis-specific ACE promoter-Cre-poly A signal; neo, an expression cassette for the neomycin-resistance gene; DT-A, MC1-DT-A-poly signal cassette. The ACN cassette consists of tACE-Cre and neo cassettes flanked by loxP sites, and this cassette is removed in the mouse testis during germline transmission. Arrowheads indicate the approximate positions of PCR primers. F2, SVloxP-3′-F2; R2, Noto-PC-3′-R2; nF, *Noto* genotype F; eF, ERT2 genotype F; nR, *Noto* genotype R.
(C-E) Southern blot analysis of homologous recombination in ES cells. Hind III-digested ES genomes were separated on a 0.3% agarose gel and blotted to nylon membranes. Hybridization with the 5′ probe (C) and 3′ probe (D) gave two bands that corresponded to the predicted lengths of the wild-type (wt) and knock-in (ki) alleles. Hybridization with the internal (neo) probe (E) gave a single band corresponding to the knock-in allele. (F) Genotype determination of $Noto^{nmCherry\text{-}CreERT2}$ mice by PCR. Note that the ACN cassette was removed in knock-in mice #1 and #4, while knock-in ES cells produced only a wild-type band, because the ACN cassette prevented PCR amplification of the mutant allele.

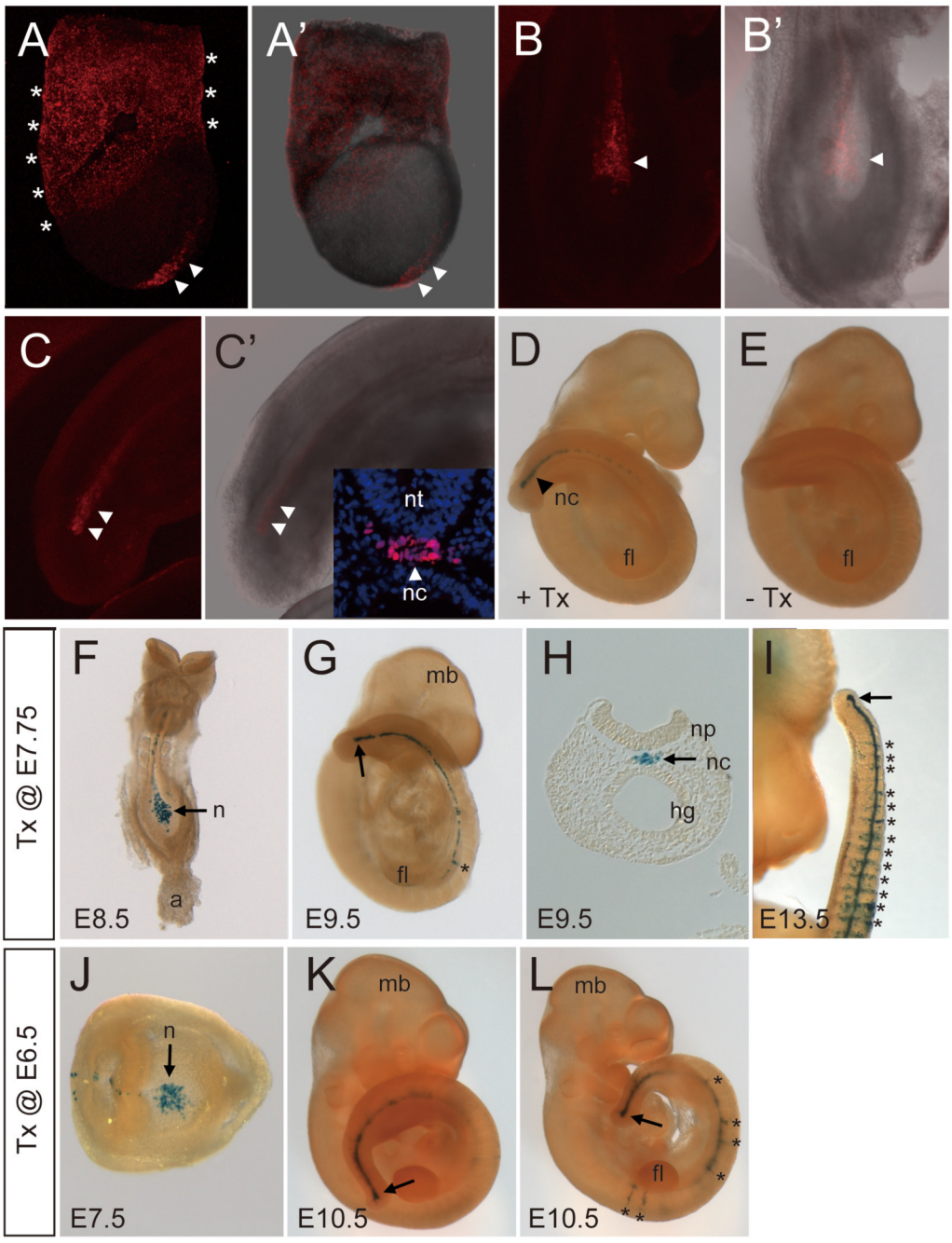

Figure 3. Genetic lineage tracing of *Noto*-expressing cells

(A-C) Expression of nuclear mCherry in *Noto*$^{nmCherry\text{-}CreERT2/+}$ embryos. The mCherry signal was observed in the nuclei of node cells and in the posterior head process (arrowheads) at E7.5 (A, A'). Stars indicate auto-fluorescence in the visceral endoderm, which was not derived from mCherry. The mCherry signal was observed in the node (arrowhead) of E8.5 embryos (B, B') and the posterior notochord-like tissue in the tail bud (arrowheads) at E9.5 (C, C') embryos. The inset in C' shows the immunofluorescence staining of mCherry protein (red) in a cross-section of E9.5 tail. Nuclei were counterstained with DAPI (blue). (D, E) Cre activity depends on Tx administration in *Noto*$^{nmCherry\text{-}CreERT2/+}$;*ROSA26*$^{lacZ/+}$ embryos. Tx administration at E8.5 induced Cre-mediated recombination in the posterior notochord by E9.5 (D), while no

recombination was observed without Tx (E). (F-I) Lineage tracing of Noto-positive cells by Tx administration at E7.75. β-galactosidase activity at E8.5 (F, ventral view), E9.5 (G, side view; H, a cross section near the posterior end of the notochord) and E13.5 (I, tail region). (J-L) Lineage tracing of Noto-positive cells by Tx administration at E6.5. β-galactosidase activity at E7.5 (J, ventral view, anterior is to the left) and E10.5 (K, L) embryos. Arrows in G, I, K and L indicate the posterior end of the notochord. Stars in G, I, and L indicate non-notochordal cells labeled with β-galactosidase.

Abbreviations: a, allantois; fl, fore limb; hg, hindgut; mb, midbrain; n, node; nc, notochord; np, neural plate; nt, neural tube.

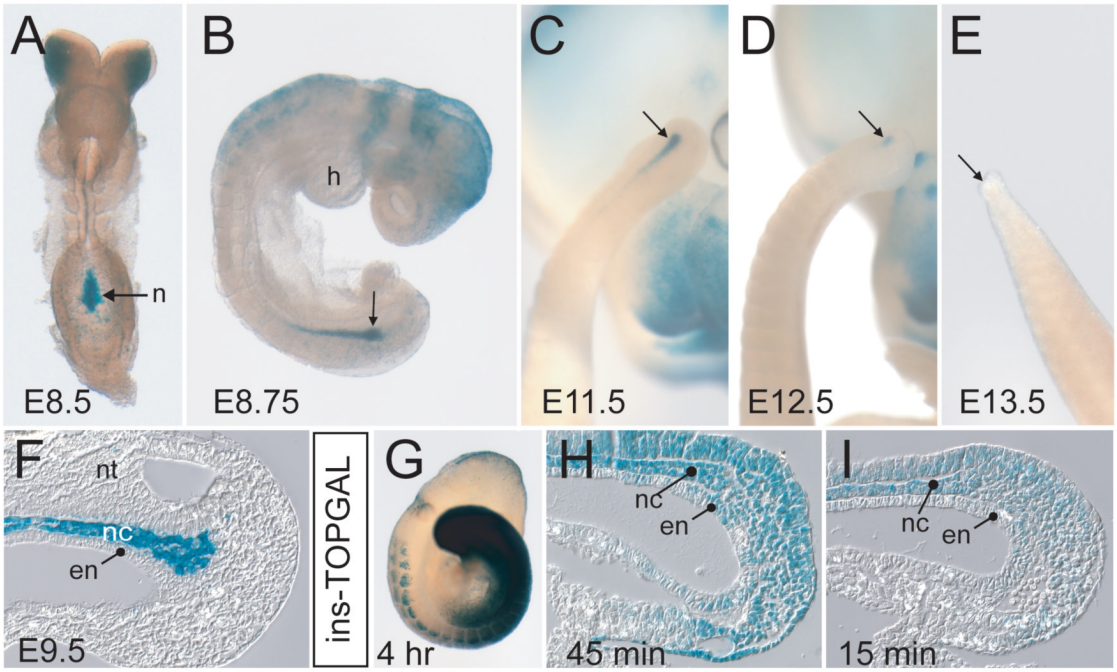

Figure 4. Activation of Wnt signaling in the NPCs

(A-E) Whole-mount β-galactosidase staining of *TOPGAL* transgenic embryos at (A) E8.5, (B) E8.75, (C) E11.5, (D) E12.5, and (E) E13.5. Arrows indicate the node or the posterior end of the notochord.

(F) Sagittal section through the tail of an E9.5 *TOPGAL* embryo.

(G-H) Whole-mount β-galactosidase staining of a ins-*TOPGAL* transgenic embryo at E9.5 and (H, I) sagittal sections through the tails of similar embryos. The color reaction was allowed to proceed for (G) 4 hours, (H) 45 minutes, or (I) 15 minutes.

Abbreviations: en, endoderm; h, heart; n, node; nc, notochord; nt, neural tube.

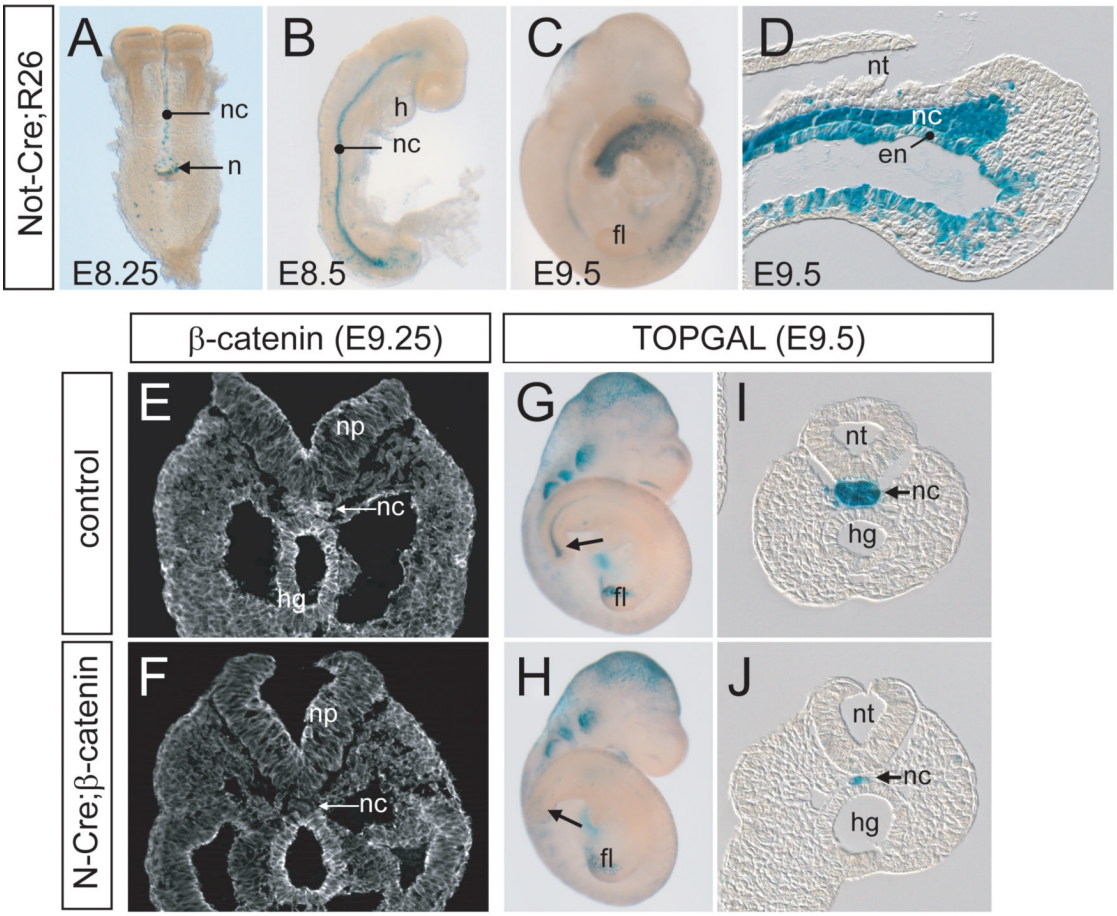

Figure 5. Attenuation of Wnt signaling by notochord-specific ablation of the *β-catenin* gene

(A-D) Whole-mount β-galactosidase staining of *Not-Cre;ROSA26* embryos at (A) E8.25, (B) E8.5, and (C) E9.5. (D) Sagittal section through an E9.5 tail.

(E, F) Immunofluorescent staining of β-catenin protein in (E) control and (F) *Not-Cre;β-catenin*$^{flox/flox}$ (*N-Cre;β-catenin*) embryos. Arrows indicate the notochord, showing the specific ablation of β-catenin.

(G-J) Whole-mount β-galactosidase staining and tail-region cross-sections of E9.5 (G, I) *TOPGAL* and (H, J) *Not-Cre;β-catenin*$^{flox/flox}$; *TOPGAL* embryos.

Abbreviations: en, endoderm; fl, forelimb bud; h, heart; hg, hindgut; n, node; nc, notochord; nt, neural tube; np, neural plate.

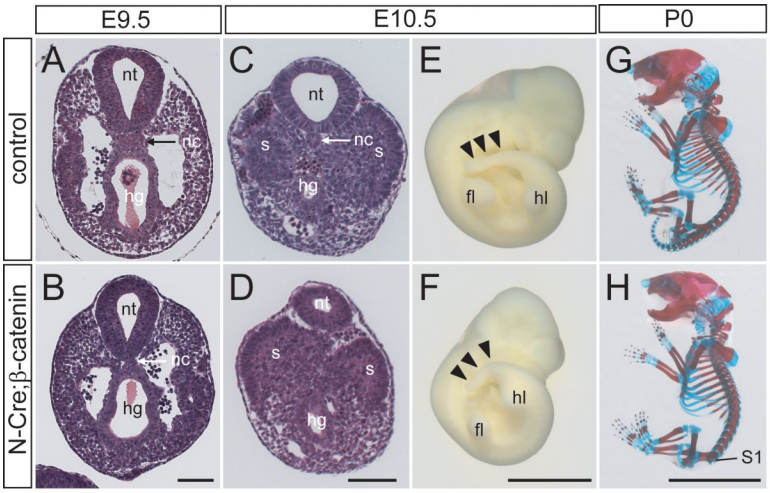

Figure 6. ***Not-Cre;β-catenin*$^{flox/flox}$ mutants lack a posterior notochord**

(A-D) Hematoxylin and eosin staining of cross-sections through the tail regions of (A, C) control and (B, D) *Not-Cre;β-catenin*$^{flox/flox}$ (*N-Cre;β-catenin*) embryos at (A, B) E9.5 and (C, D) E10.5. External morphologies of E10.5 (E) control and (F) *Not-Cre;β-catenin*$^{flox/flox}$ embryos, showing the curled and shorter tail of the mutant (arrowheads). (G, H) Skeletal specimen of (G) control and (H) *Not-Cre;β-catenin*$^{flox/flox}$ neonates (P0). The interparietal bone of the posterior skull of the control neonate was lost during the staining procedure.

Scale bars: 50 μm for A, B, C, and D; 2 mm for E, F; 1 cm for G, H.

Abbreviations: fl, forelimb bud; hg, hindgut; hl, hindlimb bud; nc, notochord; nt, neural tube; s, somite; S1, first sacral vertebra.

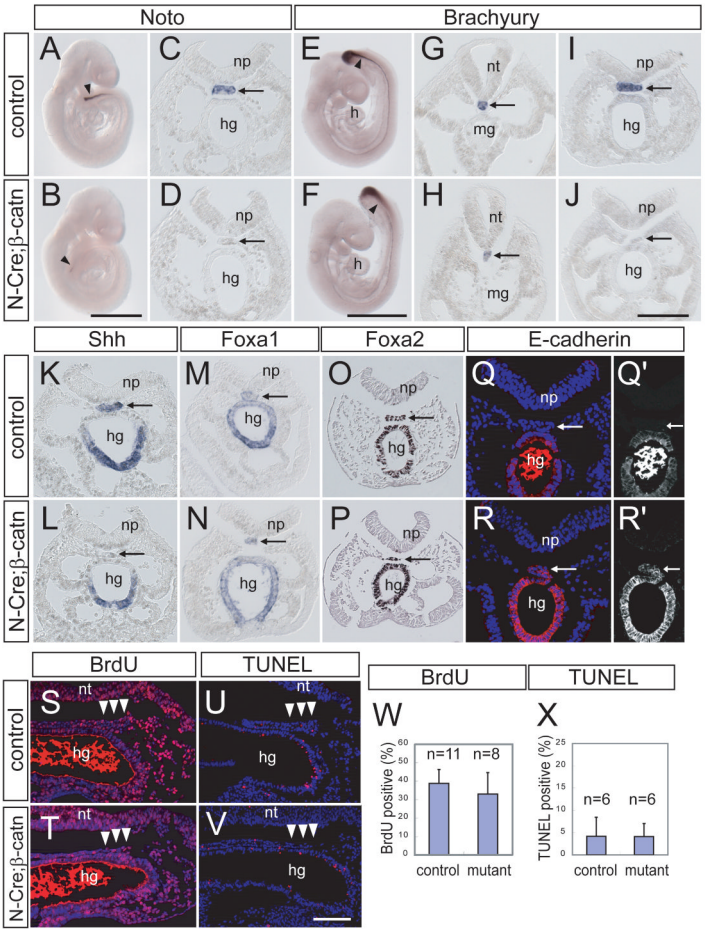

Figure 7. *Not-Cre;β-catenin*$^{flox/flox}$ embryos showed altered gene expression and unaltered cell proliferation and survival at the end of the posterior notochord

(A-V) Arrowheads indicate the posterior end of the notochord, and arrows indicate the notochord/notochord-like tissue, throughout the figure.

(A-D) Whole-mount *in situ* hybridization of *Noto* and the corresponding cross-sections through the posterior region in E9.5 (A, C) control and (B, D) *Not-Cre;β-catenin*$^{flox/flox}$ (*N-Cre;β-catn*) embryos.

(E-J) Whole-mount *in situ* hybridization of *Brachyury* and corresponding cross-sections in E9.25 (E, G, I) control and (F, H, J) *Not-Cre;β-catenin*$^{flox/flox}$ embryos. (G, H) Cross-sections through the trunk. (I, J) Cross-sections through the posterior region.

(K-N) Cross-sections through the posterior region of E9.25 (K, M) control and (L, N) *Not-Cre;β-catenin*$^{flox/flox}$ embryos stained for (K, L) *Shh* or (M, N) *Foxa1* RNA by whole-mount *in situ* hybridization.

(O, P) Immunohistochemical staining of Foxa2 on cross-sections through the posterior region of E9.5 (O) control and (P) *Not-Cre;β-catenin*$^{flox/flox}$ embryos.

(Q-R') Immunofluorescent staining of E-cadherin on cross-sections through the posterior region of E9.25 (Q, Q') control and (R, R') *Not-Cre;β-catenin*$^{flox/flox}$ embryos. Q, R: merged images with DAPI (blue), Q', R': E-cadherin only.

(S-V) (S, T) BrdU labeling and (U, V) TUNEL of the tail region of E9.25 (S, U) control and (T, V) *Not-Cre;β-catenin*$^{flox/flox}$ embryos. (W, X) Percentage of posterior-end notochord cells that were (W) BrdU-positive or (X) TUNEL-positive cells. Error bars indicate standard deviation.

Scale bars: 1 mm for A, B, E, and F; 50 μm for G-R; 100 μm for S-V.

Abbreviations: h, heart; hg, hindgut; hl, hindlimb bud; mg, midgut; np, neural plate; nt, neural tube.